CFDRC
215 Wynn Drive • Huntsville, Alabama 35805
Tel.: (256) 726-4800 • FAX: (256) 726-4806
www.cfdrc.com • info@cfdrc.com

LES SOFTWARE FOR THE DESIGN OF LOW EMISSION COMBUSTION SYSTEMS FOR VISION 21 PLANTS

Quarterly Technical Progress Report for

July 2001 – September 2001

by

Steve Cannon
Virgil Adumitroaie
Keith McDaniel
Cliff Smith

October 2001 **CFDRC Report No. 8321/4**

Contract No.: DE-FC26-00NT40975

submitted to

AAD Document Control, M/S 921-107
National Energy Technology Center
U.S. Department of Energy
P.O. Box 10940
Pittsburgh, PA 15236

Technical Monitor: Mr. Norman T. Holcombe
Contract Monitor: Ms. Crystal Sharp

West Coast Branch • 660 S. Bernardo Avenue, Suite #4 • Sunnyvale, CA 94087-1066 • Tel: (408) 524-4800 • FAX: (408) 524-5200

DISCLAIMER

ABSTRACT

Further development of a combustion Large Eddy Simulation (LES) code for the design of advanced gaseous combustion systems is described in this fourth quarterly report. CFD Research Corporation (CFDRC) is developing the LES module within the parallel, unstructured solver included in the commercial CFD-ACE+ software. In this quarter, in-situ adaptive tabulation (ISAT) for efficient chemical rate storage and retrieval was further tested in the LES code. A more efficient PK binary tree data structure is being developed and implemented to replace the original BSP-tree structure. Implementation of the Linear Eddy Model (LEM) for subgrid chemistry has also started. In addition, Georgia Tech has shown that a chemical neural net (1-step chemistry) trained at certain turbulent conditions can be used at different turbulent conditions without expensive chemical kinetic integrations. Initial evaluations of the code accuracy have also been carried out. The evaluations cases included the unstable DOE-NETL combustor and a lid-driven cavity.

Next quarter, the ISAT algorithm for efficient chemistry will be tested for the unstable DOE-NETL combustor. Initial flame calculations, with the LEM subgrid chemistry model are planned. Also, demonstration of the neural net approach, for chemical kinetics speed-up, should be demonstrated for more advanced chemistry (8-species and 19-species mechanisms).

TABLE OF CONTENTS

LIST OF FIGURES

LIST OF TABLES

1. INTRODUCTION

Vision 21 combustion systems will require innovative low emission designs and low development costs if Vision 21 goals are to be realized. In this three-year project, an advanced computational software tool will be developed for the design of low emission combustion systems required for Vision 21 clean energy plants. The combustion LES software will be able to accurately simulate the highly transient nature of gaseous-fueled turbulent combustion so that innovative concepts can be assessed and developed with fewer high-cost experimental tests. During the first year, the project will include the development and implementation of improved chemistry (reduced GRI mechanism), subgrid turbulence (localized dynamic), and subgrid combustion-turbulence interaction (Linear Eddy and Conditional Moment Closure) models into the CFD-ACE+ code. University expertise (Georgia Tech and UC Berkeley) will be utilized to help develop and implement these advanced submodels in the unstructured, parallel CFD flow solver. Efficient numerical algorithms that rely on *in situ* look-up tables or artificial neural networks will be used for the expensive subgrid chemical kinetic and mixing calculations. In the second year, the combustion LES software will be evaluated and validated using experimental data from lab-scale and industrial test configurations, including important benchmark data from DOE-NETL. During the last year, seven industrial and academic partners will take the combustion LES code and exercise it on problems of their choice. Final feedback and optimizations will then be implemented in the final release version of the combustion LES software.

2. EXECUTIVE SUMMARY

Work in this fourth quarter (July - September 2001) has included the development of a new and more efficient binary tree data structure for the in situ adaptive tabulation (ISAT) of chemical kinetics. Work has also continued on implementing the on-line Linear Eddy Model (LEM) for subgrid chemistry into CFD-ACE+. Georgia Tech has successfully trained a neural net for accurate and efficient reactions (1-step chemistry) in various turbulent environments.

Work in this third quarter has also included further improvements and testing of the parallel LES methodology in CFD-ACE+. Better processor synchronization with optimized parallel transfers has been implemented. A computational speed-up of 50 (80% efficiency) was achieved for a 64-processor LES test case. The parallel code has been tested with reduced chemical mechanisms and advanced subgrid turbulence models. A 19-species natural gas mechanism, including 31 steady-state species, was successfully used in the unstable DOE-NETL combustor case. The localized dynamic subgrid kinetic energy model provided good agreement with data in a lid-driven cavity test case.

Next quarter, implementation and testing of the following capability is planned:

1. Finish ISAT (with PK-tree data structure) implementation.

2. Test ISAT 19-species, DOE NETL combustion instability case.

3. Implement and test on-line LEM with 1-step methane chemistry in CFD-ACE+

4. Test 1-step ANN on unstable DOE-NETL case.
5. Develop 8-species and 19-species ANN for range of turbulent conditions.

3. EXPERIMENTAL

No experiments were performed this quarter.

4. RESULTS AND DISCUSSION

4.1 In Situ Adaptive Tabulation (ISAT)/Pk-Tree Data Structure

Improvement and Optimization of ISAT

As described last quarter, the original ISAT algorithm, developed by Pope (1997), was implemented in CFD-ACE+. During this fourth quarter, ISAT was tested for the 19-species mechanism on several cases including the unstable DOE combustor. Our initial results indicated that ISAT could work for small 2D cases that remained relatively stable. But, for large amplitude combustion instability cases the table size continued to grow even after the available RAM (768 MD per processor) was used up. Figure 1 shows a comparison of combustor pressure in the DOE-NETL case using ISAT versus direct integration for the 19-species chemistry. Good accuracy can be obtained with ISAT, but 80-90% of the chemical kinetic calculations were still additions (direct integration) rather than retrievals. The table fills up after ~ 2000 timesteps. Figure 2 shows results with less error control. As shown, poor results are obtained if the table is not allowed to grow.

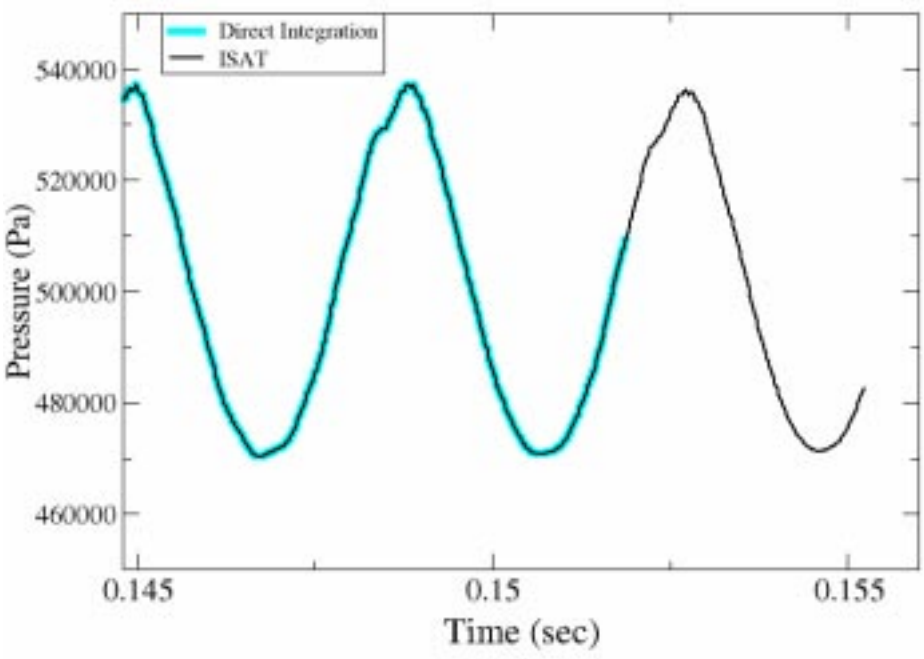

Figure 1. Comparison of ISAT (high error control) with Direct Integration for Unstable DOE Combustor

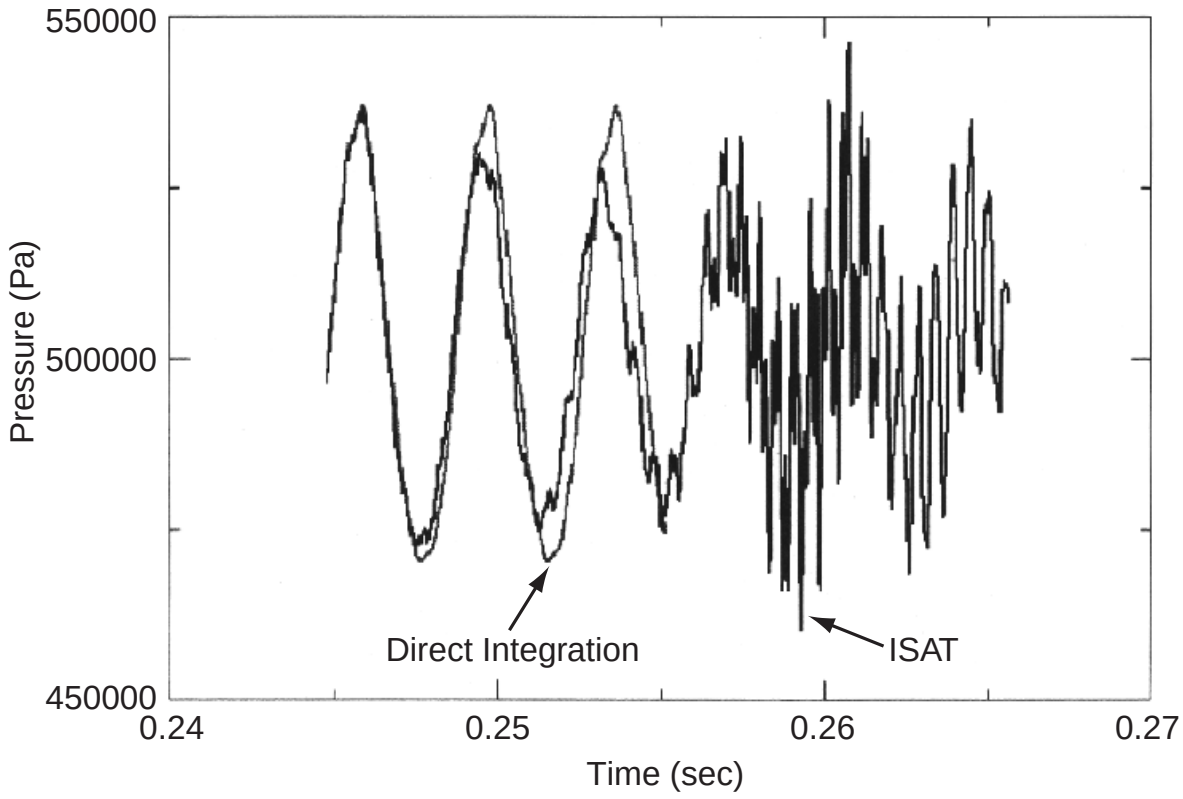

Figure 2. Comparison of ISAT (low error control) with Direct Integration for Unstable DOE Combustor

These original ISAT results indicate a previously observed problem in the binary tree data structure. That is, difficulties in locating nearest neighbor compositions and thus a duplication of records. Professor Menon at Georgia Tech has eluded to this potential problem in his recent work (Kapoor et al, 2001). Specifically, the following shortcomings with the original ISAT were identified:

a. the binary tree structure (BSP-tree) can become highly unbalanced, leading to inefficient storage and expensive searches;
b. for a given composition query the search algorithm does not guarantee the return of the nearest neighbor, thus leading to unnecessary duplication of the stored data; and
c. when the method was extended to reuse a generated ISAT table, it was found that even when starting from the same initial conditions, the algorithm added new records in the binary tree.

Based on a review of existing data structures and multi-dimensional access methods, a Pyramid K-instantiable (PK) tree was investigated and is being implemented in ISAT.

The PK-tree is described in detail by Yang et al (1997). This tree structure differs from all existing trees by using a unique set of constraints to eliminate unnecessary nodes that can result from a skewed spatial distribution of objects. This ensures that the total number of nodes in a PK-tree is O(N) and the average height is of O (log N). A remarkable set of properties of PK-trees include: non-overlapping of sibling nodes and uniqueness of the tree for a given set of data points.

Computational studies have shown that the PK-tree outperforms other methods (see Figure 3). The preliminary evaluations have shown that PK-tree can reduce storage requirements up to 50% compared to the current indexing method used in the ISAT module and allows for very efficient nearest-neighbor searches. The code is in a development/testing stage and should be fully operational in CFD-ACE+ by the next reporting period.

(a)

(b)

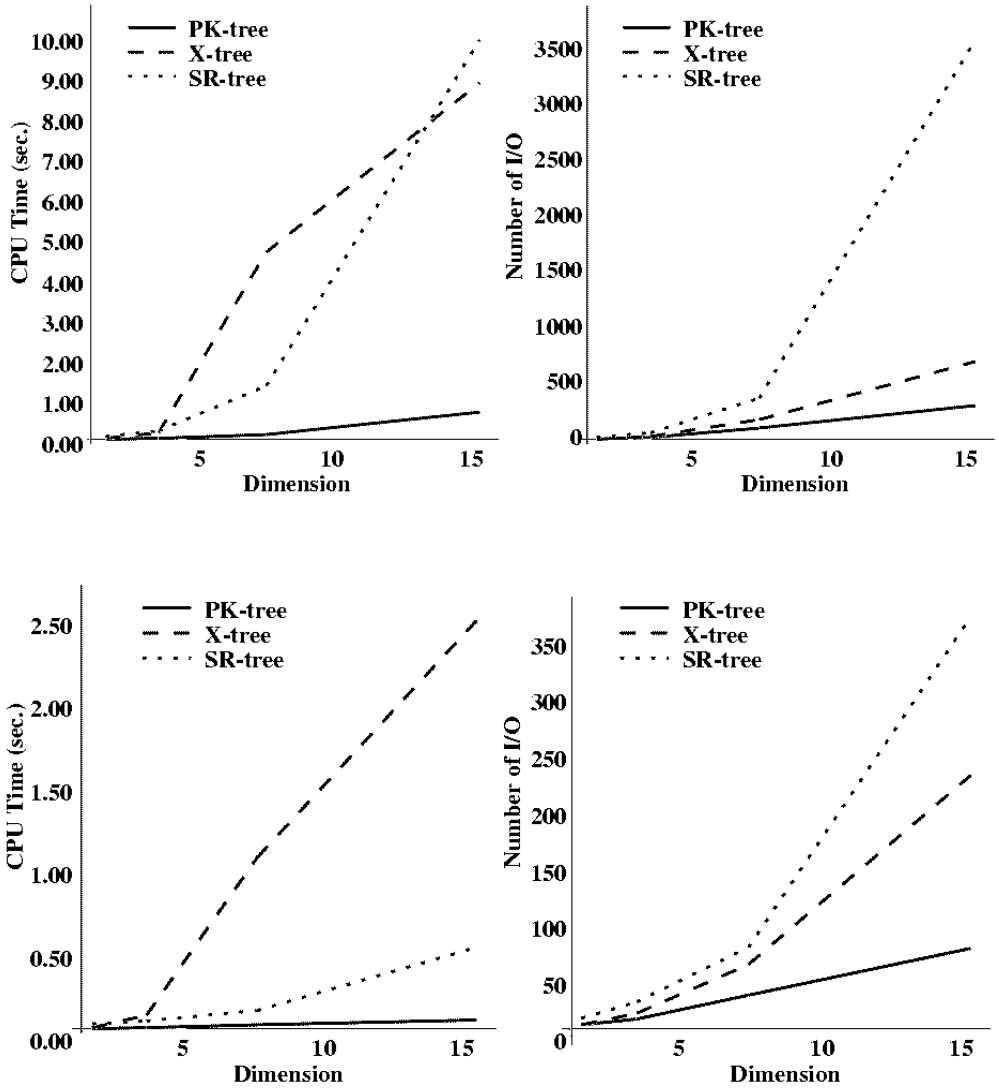

Figure 3. (a) KNN and (b) Range Query Performance for Clustered Data Distribution (Young et al, 1997)

4.2 On-Line Linear Eddy Model (LEM) Implementation

During the last quarter, CFDRC received initial subroutines from Georgia Tech for the on-line LEM. The on-line LEM is being implemented in CFD-ACE+. The on-line LEM is expensive since a neural net curve fit will not be used. The on-line LEM slices each LES cell into many smaller 1D domains. Then the species transport equation, including reaction and molecular diffusion, are solved exactly. Turbulent stirring is modeled with a stochastic pdf approach. Initial implementation and testing of the LEM with 1-step chemistry should be performed by the next quarterly report.

4.3 LEM/Neural Net Development

Artificial Neural Networks (ANN) are being developed to model detailed chemical kinetics in LES. Earlier studies (Kapoor et al., 2001) focused on a 19-species methane-air mechanism and demonstrated the feasibility of developing ANN for the thermo-chemical state. The ANN was developed and applied to a turbulent premixed flame (Flame F1) that was in the thin-reaction-zone regime. Earlier studies attempted to develop a single 20-ANN set for the 19-species and temperature. In particular, the ANN was trained using an ISAT database and the manner in which the ISAT was built and the manner of ANN training showed that small errors in the radical concentration could rapidly escalate. In order to resolve this issue, a much larger set of ANNs was developed. Preliminary effort focused on training a 20-ANN set for a single species (which implies that for this mechanism, a 400-ANN set will have to be developed). This effort is currently underway but it became quickly apparent that the MATLAB software was too slow and cumbersome to do this training. After some research, we have identified new software called NEURALWARE that appears not only more accurate but also considerably faster than the MATLAB software. We have ordered this software and will restart this training once it is installed.

In the meantime, Georgia Tech has focused on the demonstration of combining ANNs trained at various flame conditions (turbulence, equivalence ratio, etc.) and then using them to predict a different flame (for which no previous ANN existed). This demonstration will show how these ANNs can be used in an actual LES. Preliminary demonstration is now complete and is reported here.

Since the MATLAB software was not optimal, for this demonstration we decided to use simpler chemistry based on a one step CH4-air combustion reaction mechanism that involves 5 species. All other conditions were maintained the same. Two ANNs were developed: one each for Flame F1 and F3 (they differ primarily in the turbulent conditions but are both still in the thin-reaction-zone). After demonstration and validation in these flames, a new flame, Flame F2, (which is in-between these two flames), was simulated using the combined ANNs for Flames F1 and F3.

A global one-step mechanism: $CH_4 + 2\,(O_2 + 3.76\,N_2) \rightarrow CO_2 + 2\,H_20 + 2.3.76\,N_2$ with an overall rate expression for the simplified 1-step reaction mechanism as described below :

$$\omega = 1.3e08 \exp(-24358.3/T)\,[CH4]^{-0.3}\,[CO2]^{1.3}$$

was employed for this demonstration (Westbrook and Dryer, 1981).

As has been discussed previously the accuracy of the neural nets depends primarily on the accuracy of the training sets chosen, which have been obtained from the ISAT (note: ISAT also has it's own margin of accuracy, which when used for ANN training, causes the resolution errors to grow).

The ANN's were obtained using a simpler network model than previously employed (as in the 19-species mechanism). A 2-layer network is considered here, for each of the output scalars, with 10 neurons in the hidden layer. A Levenberg-Marquardt Back propagation training algorithm was employed. Also, the networks were split up on the basis of temperature for each of the output scalars, a methodology discussed before for the 19-species ANN training.

Figures 4 and 5 show respectively the instantaneous and time-averaged profiles of the major species and temperature for the F1 Flame. The ANN prediction is compared to the ISAT prediction. It can be seen that with a detailed ANN for each species, both the instantaneous and time-averaged profiles are captured very accurately. Figures 6 and 7 show respectively, the corresponding prediction for the Flame F3. Finally, Figures 8 and 9 show the corresponding prediction for the Flame F2. The last two plots are obtained by using the ANNs from F1 and F3 in a weighted manner to adjust for the difference in the condition for Flame F2. It can be seen that the combined ANNs are capable of capturing the behavior of a new flame. This is critical for actual implementation in LES where the local conditions may vary over a wide range.

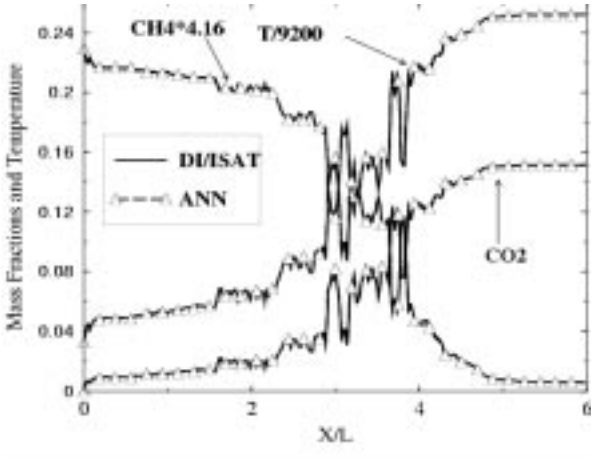

Figure 4. Instantaneous F1 Flame Profile Predicted by ANN and ISAT

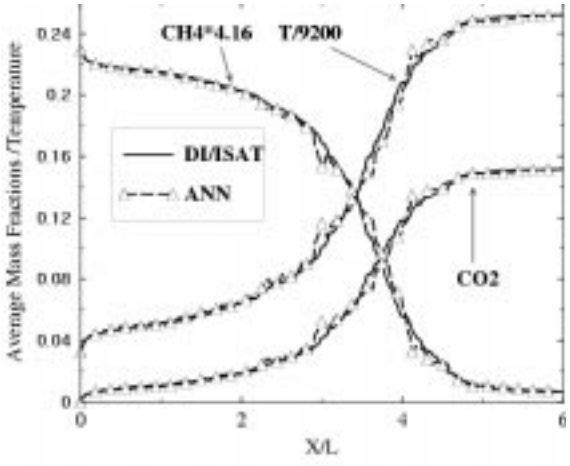

Figure 5. Time-averaged F1 Flame Predicted by ANN and ISAT

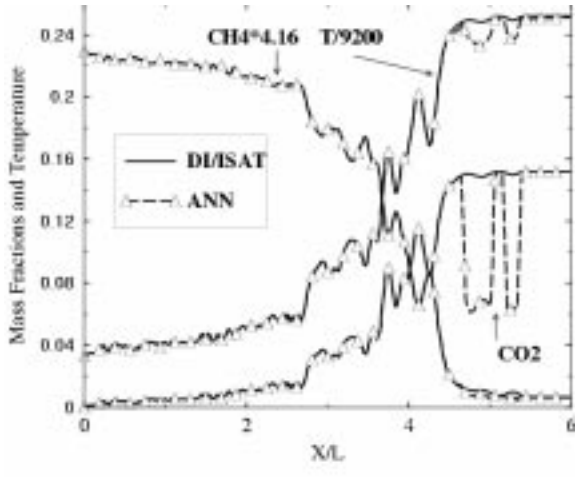

Figure 6. Instantaneous F3 Flame Profiles

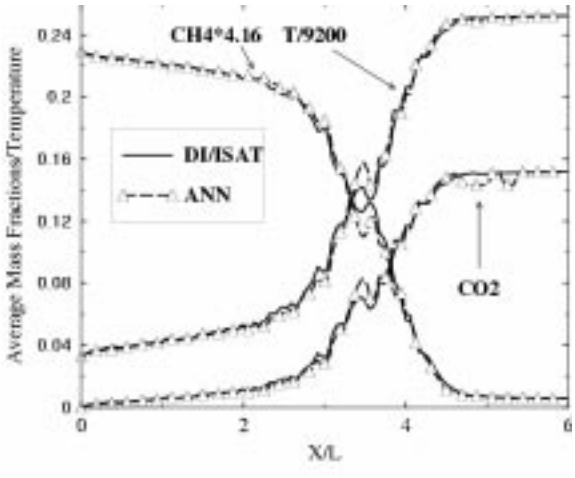

Figure 7. Time-averaged F3 Flame Profiles

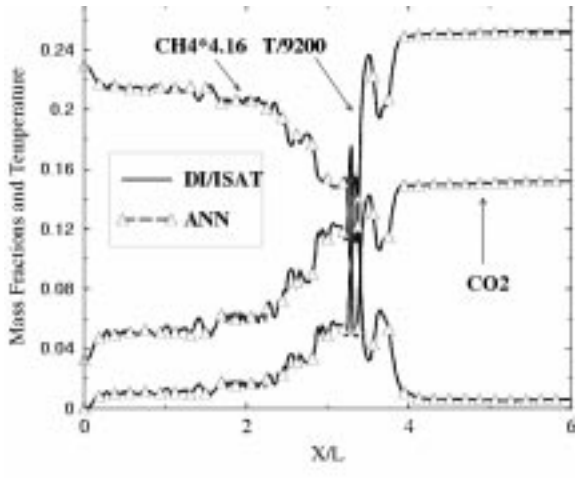

Figure 8. Instantaneous Flame F2 Profiles Predicted by Combining 2 ANNs (for F1 and F3). Results compared to direct integration by ISAT.

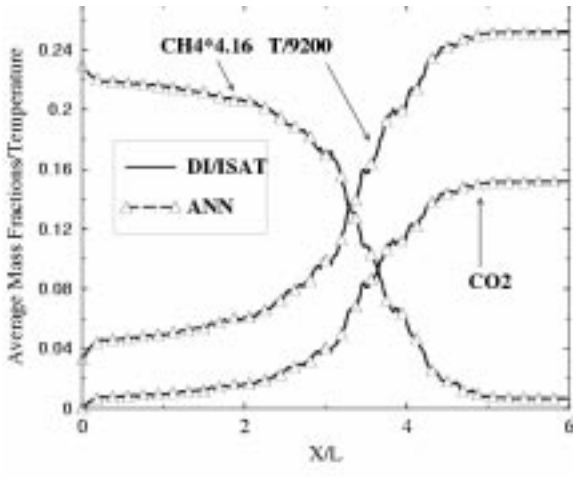

Figure 9. Time-average Flame F2 Profiles Predicted by Combining 2 ANNs (for F1 and F3). Results compared to direct integration by ISAT.

The concept of ANN for the use of prediction of the evolution of a reactive chemical scalar has been demonstrated here in particular by combining ANNs for two flames to predict a third flame. Although this test is very simple, it establishes the framework for the next more complicated ANN development for LES application. As more complex chemistry is used, especially the ones involving minor species, the order and complexity of the ANN should grow as well. This had been observed as discussed previously in the earlier studies of the ANN for the 19-species mechanism. However, the issues regarding general application with radical fluctuations needs to be carefully addressed. Therefore, for the next quarter, two parallel development efforts that are currently underway will be brought to completion. One effort focuses on the use of a combination of the thermo-chemical ANNs and turbulence ANN (for a range of equivalence ratio and turbulence

parameters) to simulate a turbulent flame using input from both these ANN sets. We plan to extend the current ANNs to include a range of length scales, turbulence intensity, and equivalence ratio and inlet reactant temperature. Once these ANNs are developed, we will use them in a combined manner to simulate a flame (or flames) for which there is no data initially. This demonstration will establish the procedure to use the "turbulent" ANN in LES since the range of conditions will cover the practical regime in a gas turbine engine. These combined ANNs can then be directly implemented into the LES code once the initial validation is completed. The second effort is on understanding the errors in radical training. Therefore, we plan to implement the new software NEURALWARE and train a 4-step, 8 species-CH4-air mechanism which will contain only one radical (H): CH_4, O_2, CO_2, H_2O, N_2, H_2, H and CO. The idea is to understand how to handle the sensitivity of the ANN to radical errors that were observed in the earlier 19-species study. Once we understand this, extension to a more complex 19-species mechanism should not pose any fundamental problem.

4.4 Improved Parallel Performance of the LES Code

The parallel performance of the LES code has been improved during the last quarter. The Linux based cluster of 64 PC's are connected through a 100 BASE-TX Ethernet Fully Connected Network Topology. The four switches are connected to a 3Com matrix module creating one virtual switch between all 64 processors. Load balancing of the communication domain, data buffering, and synchronization are parallel issues that have been found to affect the performance LES software applied on the Linux cluster.

Load balancing of the communication domain must be considered when using a large number of processors. Large synchronization times can develop if the number of neighboring processors differs for a given processor. For example, a processor with 3 neighbors will have to wait on a processor with 6 neighbors. The k-way partitioning implemented in Metis (domain decomposition software use in CFD-ACE+) minimizes the amount of transfer data but doesn't balance the number of neighboring processors. This is difficult to accomplish in a graph decomposition, but can be achieved through geometrical decompositioning. If a partitioning along an orientation axis can be achieved, then the number of neighbors for each domain will be load balanced (excluding end domains). The significant improvement in parallel performance for an x-cut decomposition versus an arbitrary (k-way) decomposition was shown in the last quarterly report for the Gosman backstep case.

The packing of ghost cell data was improved by storing a map of the ghost cell position. This increases the required memory slightly but decreases the extent of the packing loop. The loop now goes over the surface of ghost cells rather than over the total volume of cells. This has a greater effect for domains with a small surface to volume ratio.

Typical LES runs require 5-10 sweeps on the pressure correction equation for each iteration. Also, a timestep will require 5-10 iterations to obtain convergence. Previous parallel calculations transferred data at each swep within the solver for each variable to maintain an implicit solution for the entire flowfield. A zonal implicit method was then implemented (for the CGS solver) so that data transfer only occurred at the end of each iteration. This new approach slightly decreases the

solver accuracy, but for transient calculations with small timesteps (as needed for LES), the convergence can be maintained with no more than double the number of iterations per timestep.

These parallel improvements were applied to a transient simulation of a three-dimensional incompressible lid driven cavity. In order to assess parallel performance the number of timesteps, iterations, and sweeps were held constant for all runs to maintain a constant computational load. A structured grid with dimensions 191x191x95 was created for the lid driven cavity investigated by Prasad and Koseff with a SAR ratio of 0.5 (discussed in the next section). Figure 10 shows the speedup of compute time on the LES cluster. The transfer time of ghost cell data remains constant for all cases since geometrical partitioning was used to decompose the domain along the x-axis. The parallel efficiency of the 8 processor case was 98% (i.e., 2% of the total time was spent in parallel transfer). This 8-processor case was used a baseline due to RAM memory restrictions (768 MB/processor). The 8, 16, and 32 processor cases were run on 1200 MHz machines. The 64 processor case was distributed over a non-homogeneous network (8-800 MHz, 8-900 MHz) 16 1000 MHz, 32 1200 MHz). The speedup of the 64 processor case was limited by the slowest processor speed. To account for this, the 8 processor case was run on the 800 MHz processors as well. The speedup obtained for the 64 processor case was 52 which is about an 80% efficiency. The efficiency of the original parallel method (fully implicit) in CFD-ACE+ was only 60% for the same 64 processor case. The significant improvements in the parallel speedup are important for performing practical engineering LES.

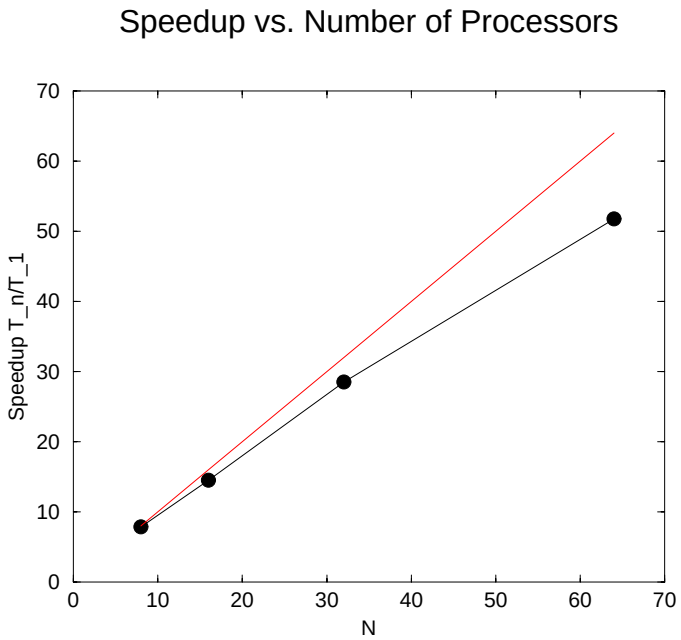

Figure 10. Speedup vs. Number of Processors

4.5 LES Code Validation - Lid Driven Cavity

Measured data from a lid-driven cavity experiment was used to validate the LES code. The Localized Dynamic Subgrid-scale Model (LDKM) was described last quarter and was used in the LES. Three-dimensional cavity flows are highly non-homogeneous with complicated flow patterns; consisting of a primary vortex and several corner vortices. The localized SGS model, such as LDKM, should be capable of predicting these flows (Menon, 1997). An experiment of a rectangular lid-driven cavity with benchmark quality data was performed by Prasad, et al. (1988). Their experiments show that local and global three-dimensional features are present in the flow. The cavity with an SAR (SAR = L/B) of 0.5:1 and a Reynolds number equal to 10,000 ($Re=U_bB/v$) was used for the validation of the LDKM model with LES (see Figure 11 for dimensions).

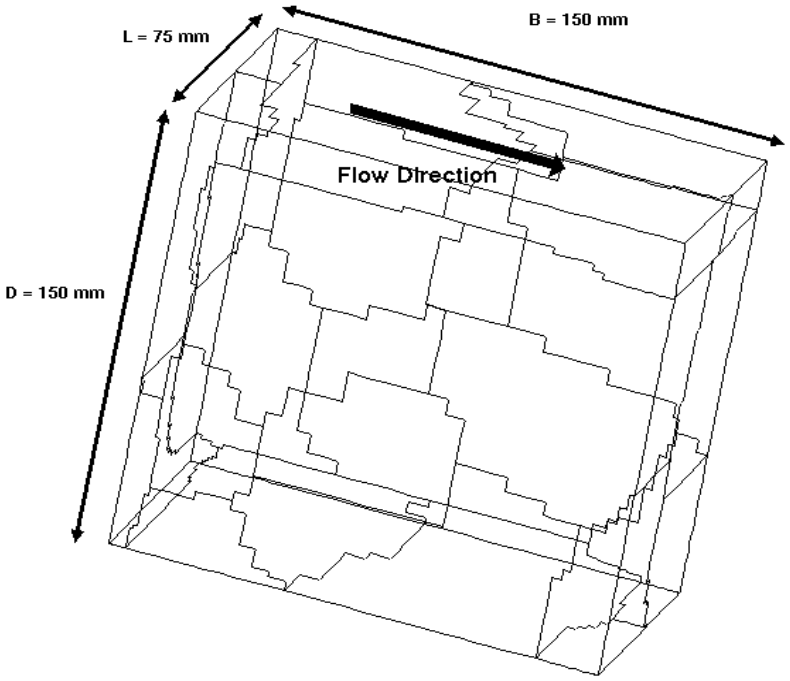

Figure 11. Lid-Driven Cavity Dimensions

The resolution of the computational grid was 64x64x32 (123039 cells). The grid was uniform in the Z direction and stretched towards the walls in the X and Y directions. A hyperbolic tangent distribution was used for the X-Y stretching with a 3.14e-4 meters spacing at the walls. The computational grid in the X-Y plane of the cavity is shown in Figure 12. The following flow conditions were specified as:

U_b = .06 m/s
T = 298.15 K
ρ = 997 Kg/m^3
Cp = 4184 J/Kg-K

Isothermal boundary conditions were used for all the walls including the lid. The U_b was imposed on the top wall to simulate the moving wall in the experiment.

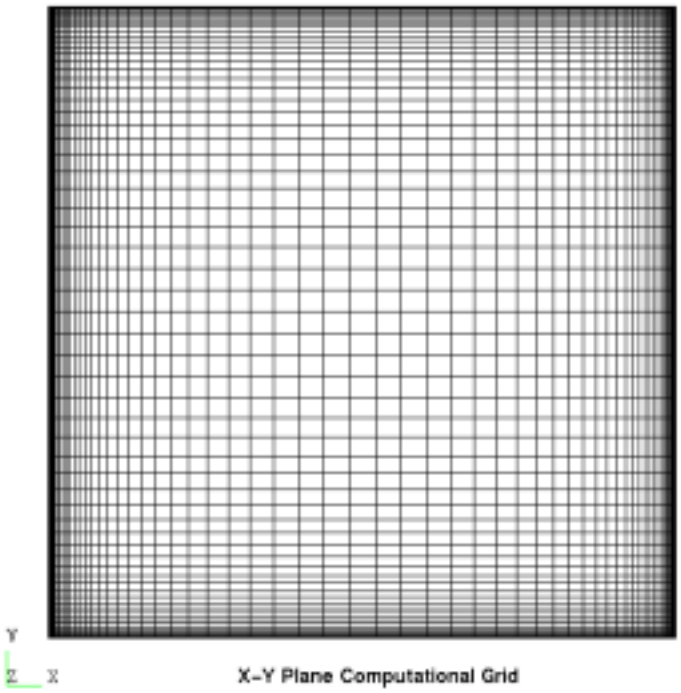

Figure 12. X-Y Computational Grid at Z = 37.5 mm

First a steady RANS solution was obtained and used as the initial condition for the unsteady RANS and LES calculations. The R grid parameter at the X-Y midplane is shown in Figure 13. This parameter is a measure of the quality of the grid for LES. A value less than zero implies that the filter or resolved scale is larger than the local energy containing scales, while a value greater than 1 implies that the resolved scales are smaller than the energy containing scales. Figure 13 shows that most of the grid is suitable for the LES calculation. The parameter is a function of the turbulent kinetic energy and is therefore dependent on the turbulence model. The parameter near the walls becomes less accurate for the RNG turbulence model used for this steady calculation. The grid parameter suggests more resolution is needed near the walls and along the top wall where large strain occurs due to the imposed velocity. Currently a 192x192x96 grid is being simulated to address this resolution issue.

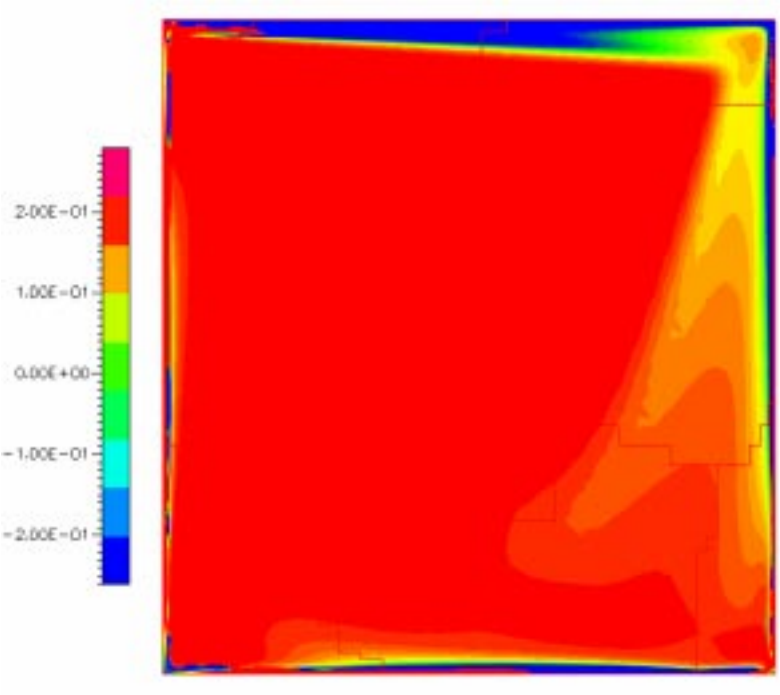

Figure 13. LES Grid Parameter

The RNG k-ε turbulence model was used for the unsteady RANS calculation and the LDKM with dynamic coefficients was used for the subgrid closure in the LES calculation. Figure 14 shows the normalized mean U-velocity along the Y-centerline.

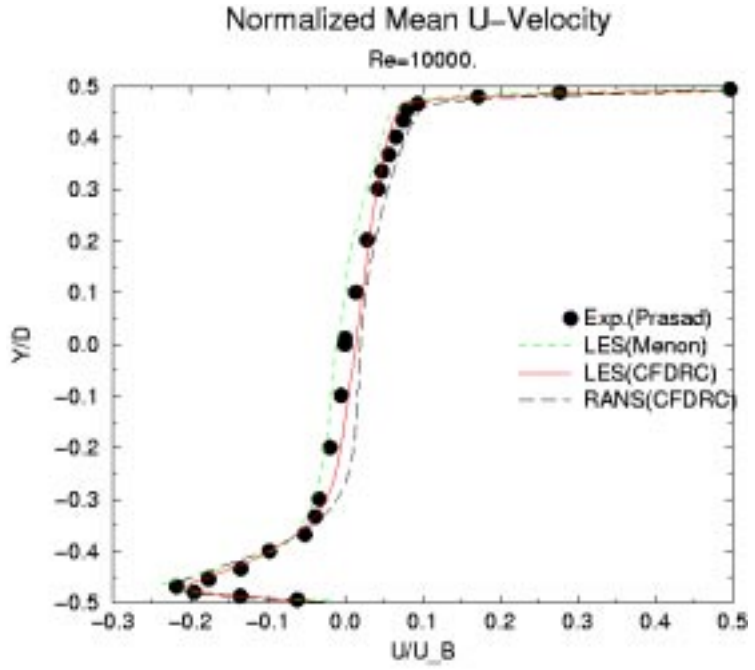

Figure 14. Normalized Mean U-Velocity

Both the LES and RANS calculations capture the mean velocity at the lower boundary wall. The LES predicts the mean velocity in the core flow and along the top wall better than the RANS calculation. This LES calculation is consistent with the LES calculation performed by Kim and Menon. Good comparisons were obtained for the mean V-velocity shown in Figure 15.

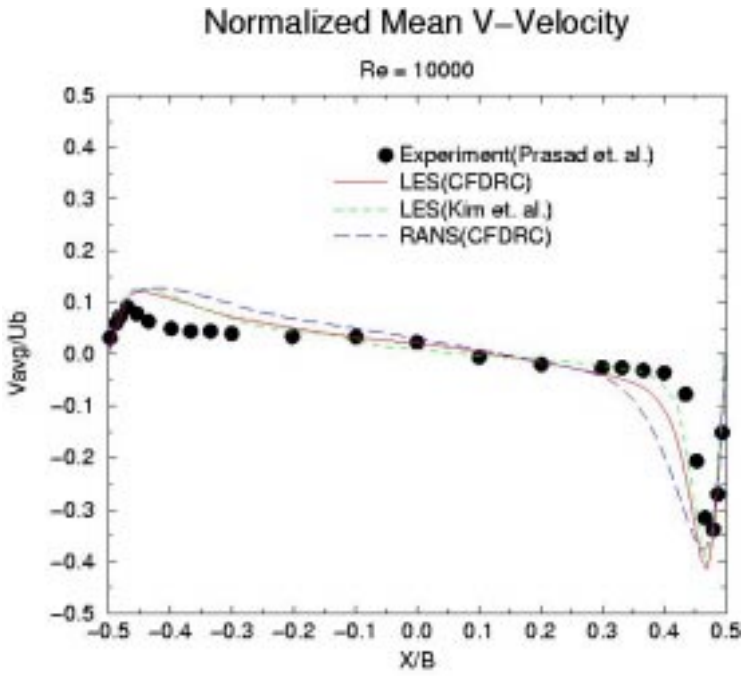

Figure 15. Normalized Mean V-Velocity

The RANS calculation over predicts the mean V-velocity at the end walls. The LES by CFDRC better predicts the overall mean V-velocity but does not show as good agreement as Kim et al. near the location of X/B = .375. Both LES models over predict the peak mean V-velocity values. The Normalized U-RMS is shown in Figure 16.

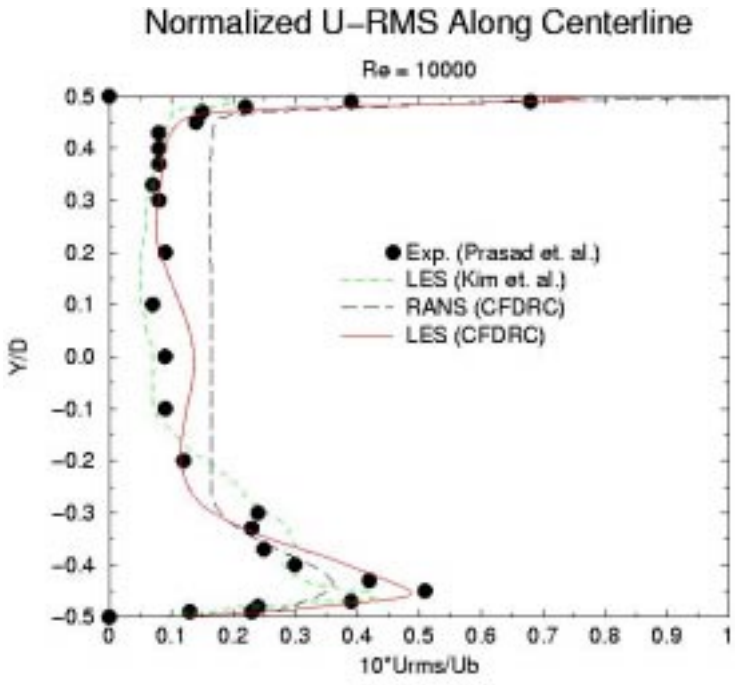

Figure 16. Normalized U-RMS Along Y-Centerline in Midplane

The LES simulations by CFDRC better predicts the U-RMS at the bottom wall compared to the LES by Kim et al., and the RANS simulation by CFDRC. It also compares better to data near the lid than that of Kim. The U-RMS near the center peaks at .15 for the LES-CFDRC simulation. This was not observed in the experiment or calculations by Kim (1997). This indicates that a longer compute time may be needed to average out the effects of the initial conditions provided by the RANS solution. Also the second peak was not captured at Y/D = -0.3. This second peak on rms could be due to the "coherent" structures described by Prasad (1989). Figure 17 shows the average U-velocity and vectors in the X-Y plane located at Z=.0375 meters and t=234 s. This shows the primary vortices and the secondary corner vortices located along the lower boundaries. A monitor point was placed 5 mm from the lower wall boundary layer to compare the U-velocity spectrum with experimental data shown in Figure 18.

The Kolmogorov -5/3 law was observed in the experiment in the inertial subrange, where the transfer of energy is dominant. The LES calculation predicts the -5/3 law observed in the experiment, which is crucial for LES calculations. The roll off in the viscous range was predicted by CFD-ACE+ at the frequency of about 0.5 Hz. The roll off is greater for the LES calculation than observed in the experiment. This indicates that higher frequency structures are dissipated more than observed in the experiment. Larger simulation times are needed to properly get statistics for the lower frequencies. This shows that LES with the subgrid scale model LDKM in CFD-ACE+ can be used to capture complex flows of three-dimensional cavity-driven flows where coherent structures may exist.

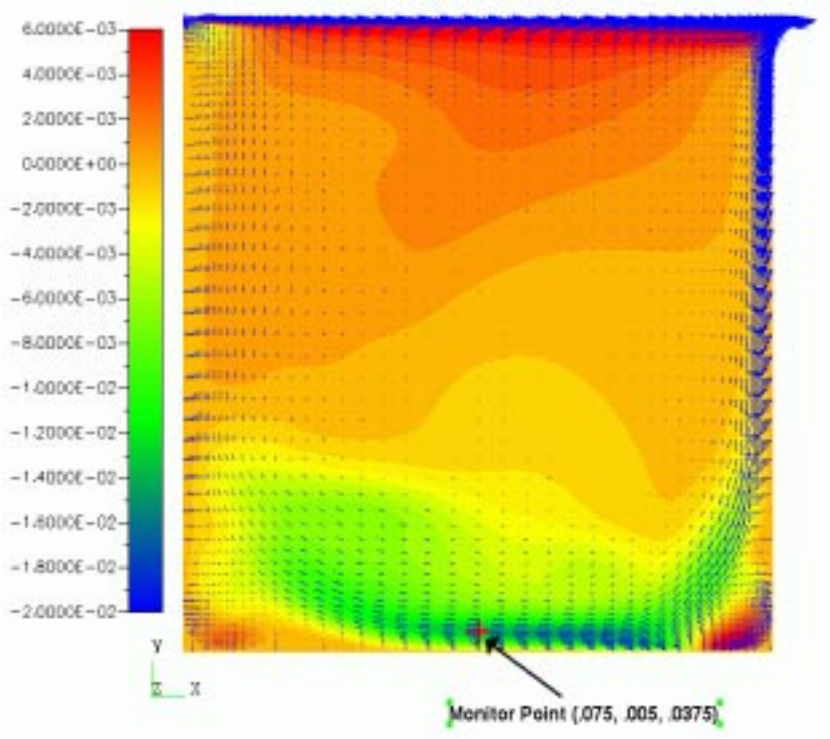

Figure 17. Average U Velocity Contours and Vectors

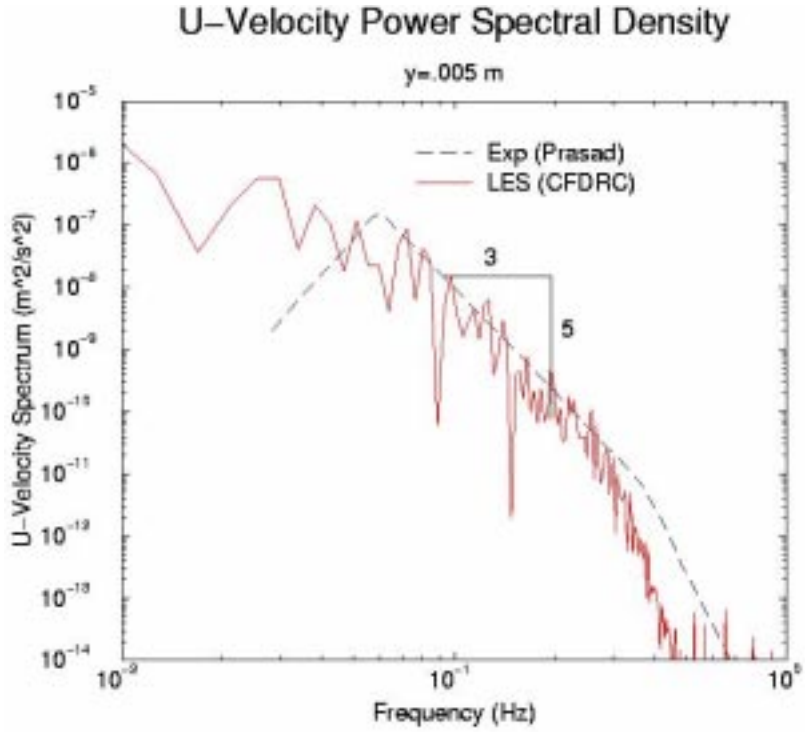

Figure 18. U-Velocity Power Spectrum

4.6 Reduced Mechanism Implementation in CFD-ACE+ (DOE NETL Unstable Combustor)

This quarter the capability of predicting instability using reduced chemical kinetic mechanisms was demonstrated. As described in the last report, the chemical kinetic mechanisms were developed by Prof. JY Chen of UC Berkeley using his computer automated reduction method (CARM). A 19 species methane mechanism was developed from a combined full mechanism for natural gas combustion. The full chemistry consisted of the GRI2.11 mechanism and a newly developed mechanism from Miller for NO. The combined mechanism more accurately describes NO emissions at rich conditions compared to the stand-alone GRI mechanism.

The 19 species mechanism consists of the following 15 global steps:

(1) H + HO2 = H2 + O2
(2) H + H2O2 = H2 + HO2
(3) 2OH = H2 + O2
(4) OH + CH3 = H2 + CH2O
(5) H + CH4 = H2 + CH3
(6) H + OH + CO = H2 + CO2
(7) 2H = H2
(8) CH2O = H2 + CO
(9) H + O2 + HCN = H2 + CO + NO
(10) O2 + C2H2 = H2 + 2CO
(11) OH + C2H4 = H2 + CH3 + CO
(12) C2H6 = H2 + C2H4
(13) H + OH = H2O
(14) H + CO + N2 = NO + HCN
(15) 2H2 + OH + NO = 2H + O2 + NH3

Thirty-one species are assumed to be at steady-state, so their full transport equation is not needed. But, their concentrations must be computed from the tracked (non-steady-state species) in order to compute the elementary rates. This inner iteration requires more computational time than standard Arrhenius mechanisms, but the accuracy is typically better. Also, the reduction in the number of species from 50 to 19 is significant in terms of memory requirements for the LES code and for chemical look-up tables.

The computations that are reported here were done with direct integration. The chemistry was handled with operator splitting, where a stiff ODE solver was used to accurately represent the simultaneous set of chemical kinetic equations. Also, in order to provide more efficient solutions, the chemical reaction rate solutions were staggered one time step during the LES. This means that the reaction rates were computed during the last iteration of the previous time step and were then used during the subsequent time-step without updates. This procedure provided robust convergence, but more importantly required only one reaction rate calculation per time step instead of the usual seven. Since small time steps were taken, the error from staggering the chemistry was assumed to be small. Figure 19 shows predicted axial velocity near the DOE combustor centerline

and at X=0.22 m for direct integration with and without staggered chemistry. The results do show a negligible effect of staggering the chemistry.

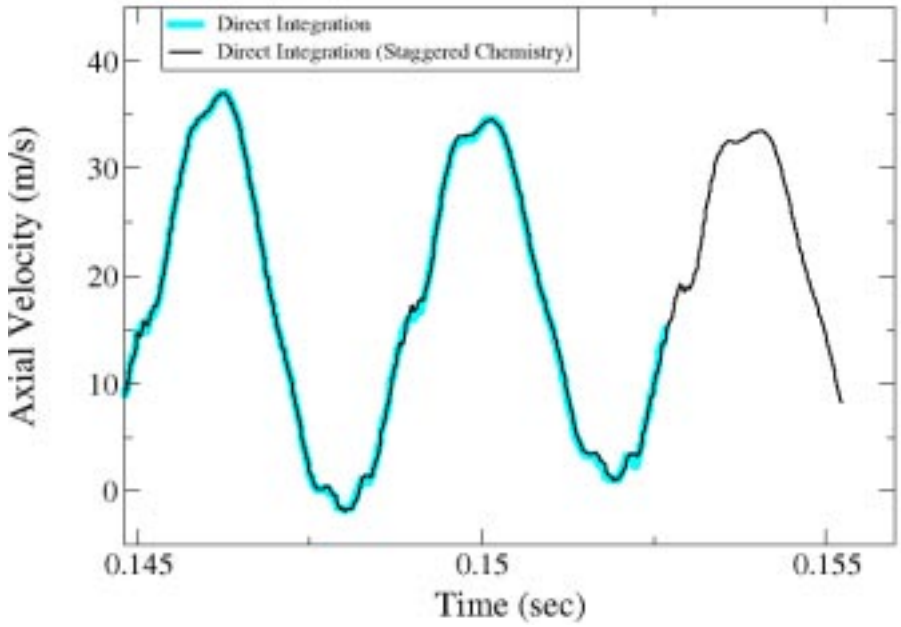

Figure 19. DOE NETL Unstable Case Predictions (X=0.22 m, Y=0.0 m) Using Direct Integration with and without Staggered Chemistry (19-species natural gas mechanism)

Unsteady RANS calculations were performed for the 2D axisymmetric DOE combustor geometry that was described in the last quarterly report. The transient calculations were started from a steady-state using a 1-step mechanism. CFD-ACE+ allows multi-step chemistry modeling when a species-by-species solution technique is utilized. This species-by-species option requires solution of the transport equation for each of the participating species (19 in this case). The 2D grid was decomposed into 13 domains and parallel computations were performed in parallel on CFDRC's cluster of Linux-based PC's.

Figure 20a shows the unstable limit cycle of pressure inside the combustor. A 6.5% pressure oscillation is observed. The Discrete Fourier Transfer (DFT) of the signal is shown in Figure 20b and clearly indicates a strong oscillation at 258 Hz. Table 1 shows the oscillation results for the experiments compared to predictions using the previous 1-step mechanism and the current 15-step mechanism.

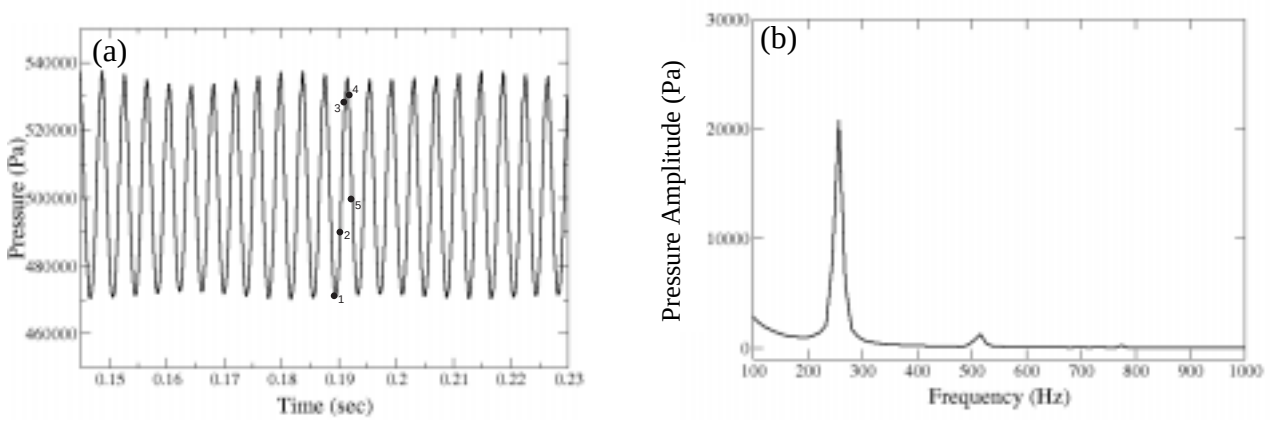

Figure 20. (a) Predicted Combustor Pressure History and (b) Corresponding Spectrum Using 19 Species Chemistry

Table 1. Predicted and Measured Oscillations in the Unstable DOE-NETL Case

	Magnitude	Frequency
Measured	6.4%	225 Hz
15-Step Chemistry	6.5%	257 Hz
1-Step Chemistry	6.8%	256 Hz

These results show that the chemistry does not have a strong effect on the predicted oscillation. This is likely due to the strong driving mechanism of a convective time-lag from the fuel injection location to the flame zone. The chemical times are certainly much smaller than the convective transport times and therefore have a very small effect on the predicted instability. The more detailed chemistry will provide superior results if strong extinction/ignition effects are present and if accurate emissions are needed. These results do show that the 15-step reduced chemistry is implemented correctly in the LES code and that successful convergence can be obtained for this unstable combustion case.

Instantaneous snapshots of pollutant emissions can be observed during the instability cycle. The predicted CO mass fraction during the oscillation cycle is shown in Figure 21, while the NO mass fractions are shown in Figure 22.

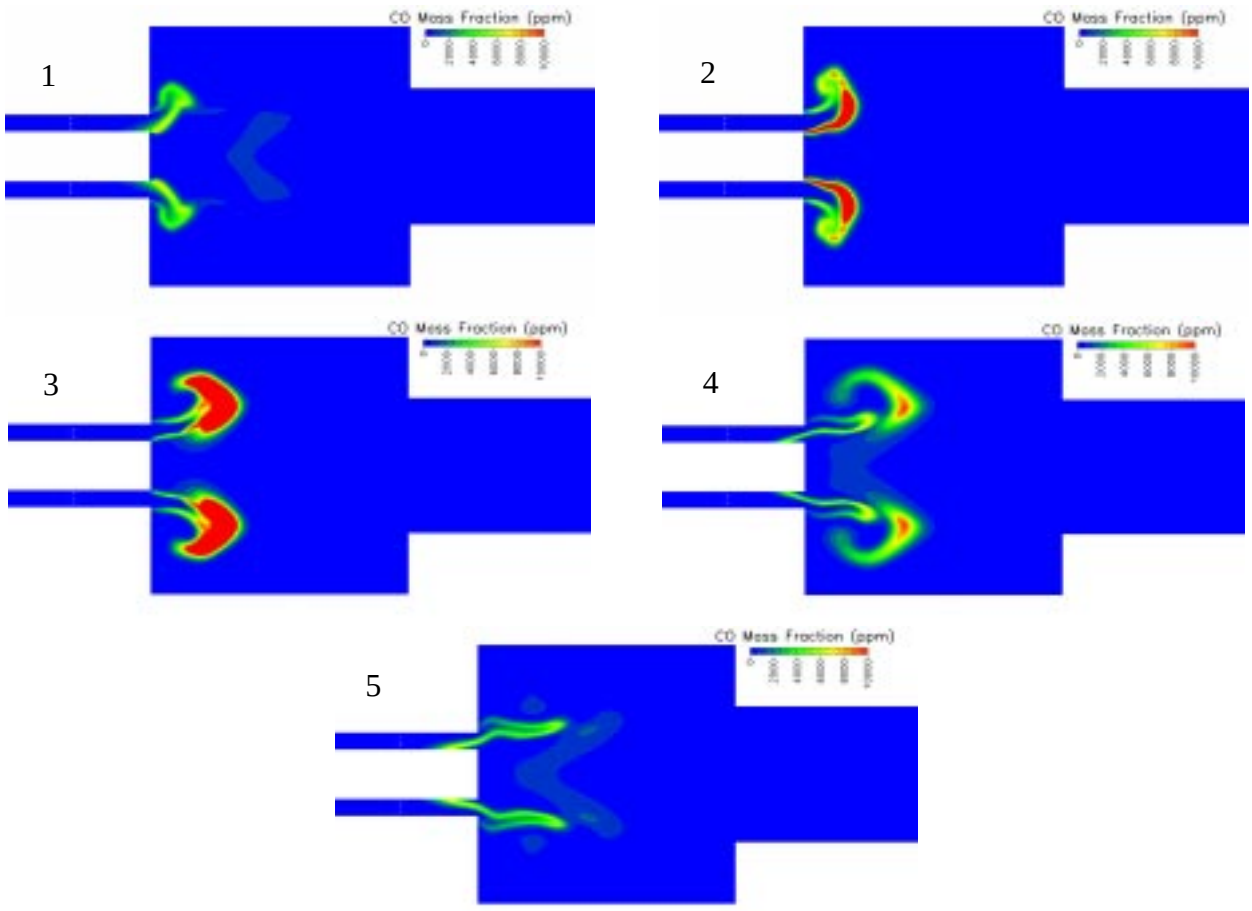

Figure 21. Predicted CO Mass Fractions During the Unstable Cycle [Unsteady RANS with 19 Species Chemistry]

The CO mass fraction contours show significant regions of high CO during the high pressure portion of the cycle. At the low pressure portion of the cycle, the CO regions are collapsed towards the centerline and are much smaller. It is known that maximum heat release occurs when CO and other intermediates are oxidized. It is very likely that maximum heat release would occur between points 3 and 4 in the cycle when the peak CO at time 3 oxidizes to significantly lower values at time 4. It is also interesting to observe a separated region of high CO at point 4 in the cycle. This separation occurs due to the high shearing that occurs during the oscillation. The unstable flow shows a strong flapping motion in the axial and radial directions. The instantaneous mass fractions of NO are also interesting. It is clear that regions of peak NO occur over much broader regions since oxidation of NO is negligible at lean conditions. Also, the peak NO occurs downstream of the peak CO regions due to the slow thermal NO formation reactions. Maximum NO regions are in the central recirculation zone where residence times are long. The outer recirculation zone is cooler and does not show as much formation of NO.

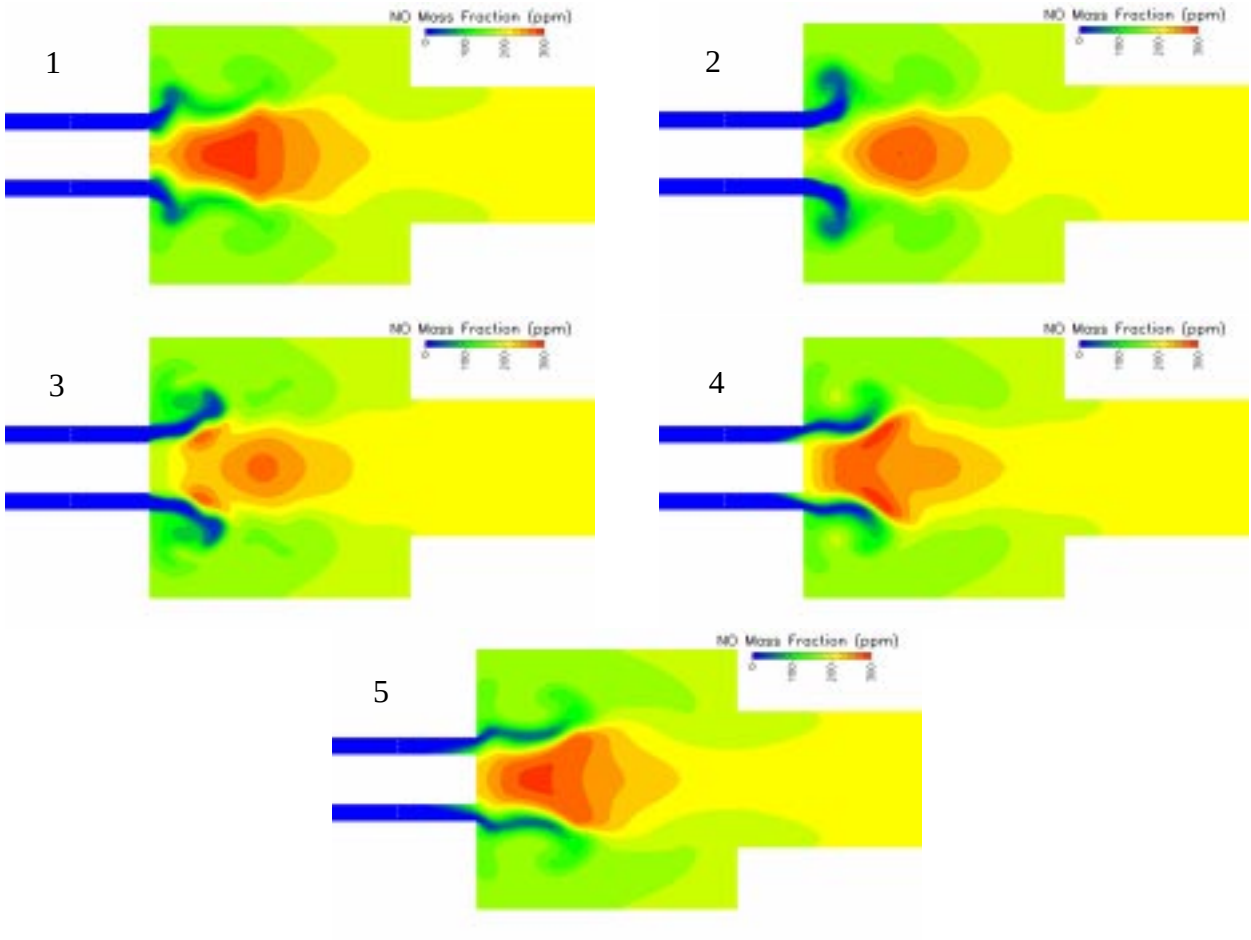

Figure 22. Predicted NO Mass Fractions During the Unstable Cycle [Unsteady RANS with 19 Species Chemistry]

In addition to the 19 species reduced mechanism, a skeletal mechanism containing 84 elementary reactions from the GRI mechanism was also tested in the LES code. This mechanism does not require the expensive inner iteration on steady-state species, but does require the solution of 21 species equations and is not as accurate as the 19 species reduced mechanism. It was found that computational times were twice as fast as the 19-species mechanism calculations. Despite this improvement in speed, the computational time was still too slow since it would take ~ 40 days for a full 3D case. The ability to replace direct integration with table look-up must be accomplished in order to produce practical run times.

4.7 Selection of Test Cases

Test cases for evaluating the LES combustion code were examined. The new experimental data from the DOE-NETL swirl combustor (Maloney et al, 2000) will be one of the test cases since it will include a comprehensive data set (velocity, species, temperature, dynamic pressure) over a large range of conditions, including high pressure. DOE-NETL has developed these experiments with well defined acoustic boundary conditions that will be needed for evaluating the code. Another data set of interest will be the lean premixed, swirling combustion data of Gore et al

(2001). This Purdue data was acquired through a DOE-ATS contract for validating gas turbine combustion CFD codes. They cover a range of flow rates including stable and unstable combustion. They also capture instantaneous images of flame structure throughout the unstable combustor cycle. These images will be valuable validation of the LES capability for predicting instability. GE and Fluent are currently using the Purdue DOE data for evaluating their combustion codes.

The low pressure data of Pitz et al (1998) will be used to validate the emissions capability of LES. They have detailed NO and CO measurements at sub 10 ppm levels. This bluff-body lean premixed data will provide a strong test of the code.

These cases will be presented in detail at the consortium meeting in January 2002. Other possible cases may be considered, depending on feedback from the participants.

5. CONCLUSION

The combustion LES code has been further developed and tested for predicting turbulent reacting flows. The LES code can now handle reduced mechanisms (19-species from GRI2.11) and has been optimized in its parallel performance. A better ISAT algorithm, with the PK-tree structure, will be needed to efficiently represent 19-species mechanisms in the LES code. The artificial neural net (ANN) approach can be used to represent chemistry at untrained conditions and will be needed for handling multi-step chemistry interactions with subgrid turbulence (i.e., 19-species LEM). The code, in its current state, can represent isothermal flowfields and combustion instability driven primarily by a fuel time lag. The code needs to be further evaluated for predicting emissions and instability due to vortex shedding on unsteady feed wakes (i.e., no fuel time lag).

6. REFERENCES

Cannon, S.M., McDaniel, K.S., and Smith, C.E., "Sensitivity Analysis of Combustion Dynamics Using Time-Accurate CFD Modeling," AIAA 2001-3971, 37th AIAA/ASME/SAE/ASEE Joint Propulsion Meeting, Salt Lake City, UT, July 8-11, 2001.

Kapoor, R., Lentati, A., and Menon, S. (2001), “Simulations of Methane-Air Flames using ISAT and ANN,” 37th AIAA Joint Propulsion Conference, Salt Lake City, UT, July 8-11, 2001.

Kim, W. and Menon, S., (1997), "Application of the Localized Dynamic Subgrid-Scale Model to Turbulent Wall-Bounded Flows", AIAA paper 97-0210.

Pope, S.B., (1997), “Computationally Efficient Implementation of Combustion Chemistry using In Situ Adaptive Tabulation,” *Combustion Theory and Modeling*, Vol. 1, pp. 41-63.

Prasad, K., and Koseff, R., (1989), "Reynolds Number and End-wall Effects on a Lid-driven Cavity Flow", Phys. Fluids A, Vol. 1, No. 2, February 1989.

Richards, G.A. and Janus, M.C., (1997), “Characterization of Oscillations During Premix Gas Turbine Combustion,” Presented at the *International Gas Turbine and Aeroengine Congress and Exhibition*, 97-GT-244, Orlando, FL, June 2-5, 1997.

Westbrook, C.K. and Dryer, F.L., (1981), Combustion Science and Technology, Vol.27, pp.31-43.

Yang, J., W. Wang, and R. Muntz (1997). Yet another spatial indexing structure. UCLA Computer Science Department Technical Report #970040. http://dml.cs.ucla.edu/,weiwang/paper/TR-97040.

APPENDIX A — WORK SCHEDULE

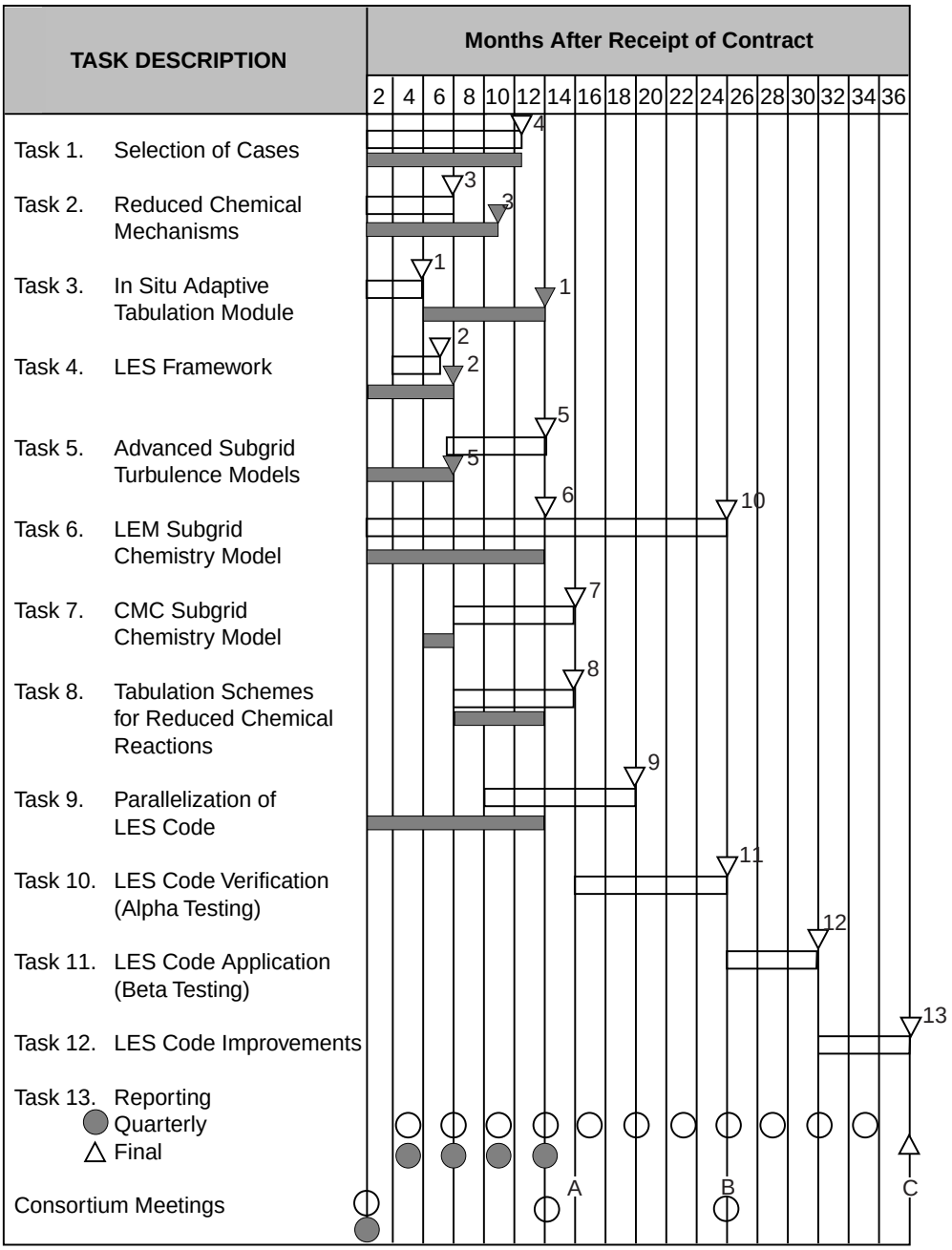

Key Milestones

1 Complete In-Situ Adaptive Tabulation Module
2 Complete LES Framework Modification to CFD-ACE+
3 Complete Reduced Mechanisms
4 Complete Selection of Cases
5 Complete Implementation of Turbulence Models
6 Complete Implementation of Initial Version of LEM Model
7 Complete Implementation of CMC Model
8 Complete Tabulation Schemes
9 Complete Parallelization of LES Code
10 Complete Implementation of LEM Model
11 Complete Alpha Testing of LES Code
12 Complete Beta Testing of LES Code
13 Final Release of LES Code

Performance Targets

A Alpha Release of LES Code
B Beta Release of LES Code
C Final Commercial Release of LES Code

Planned
Performed

APPENDIX B — FUTURE PLANS

During the next quarter, the following work is planned:

1. Test ISAT with 19 species chemistry on DOE-NETL combustion instability case.

2. Implement On-Line LEM in CFD-ACE+.

3. Develop ANN (8-species and 19-species) that can be used to predict combustion instability in DOE-NETL test case.

4. Initiate code validation using Pitz et al bluff-body data.